minerals

MDPI

Article

Characterisation and Environmental Significance of Glauconite from Mining Waste of the Egorievsk Phosphorite Deposit

Natalia Kalinina [1,*], Prokopiy Maximov [1], Boris Makarov [1], Evan Dasi [1] and Maxim Rudmin [1,2,*]

[1] Division for Geology, School of Earth Sciences & Engineering, Tomsk Polytechnic University, 634050 Tomsk, Russia; pnm1@tpu.ru (P.M.); de01@tpu.ru (E.D.)
[2] Institute of Environmental and Agricultural Biology (X-BIO), University of Tyumen, 625003 Tyumen, Russia
* Correspondence: kalininatalia58@gmail.com (N.K.); rudminma@tpu.ru (M.R.)

Abstract: This article presents the results of a study of glauconite obtained from phosphate rock waste. The aim is to study the morphological, structural and chemical characteristics of glauconite and to determine the potential for secondary use of mining waste in the agricultural sector. The electromagnetic separation method was used to obtain glauconite concentrate. The optimum parameters for obtaining the maximum mineral content in the concentrate were determined. Studies have shown that glauconite is characterised by globular, granular grains of the highly mature variety. Glauconite almost invariably contains inclusions of pyrite and apatite, which significantly improve the characteristics of the fertiliser. Laboratory experiments have shown that glauconite waste and glauconite concentrate have a positive effect on plant growth and development. The high potassium content, the favourable globular shape of the grains, and the presence of apatite and pyrite inclusions indicate the potential use of glauconite from mining waste as a potash fertiliser. Application of glauconite fertiliser to the soil will provide an opportunity to improve its texture, providing better moisture and aeration. The use of glauconite fertiliser is particularly valuable on acidic soils where apatite can be dissolved, making phosphorus available to plants. This nutrient additionally favours plant growth, as well as reducing the risk of heavy metal accumulation in the soil. Thus, glauconite from the waste of the Egorievsk deposit represents a promising fertiliser for improving soil quality and increasing crop yields.

Keywords: glauconite; waste rock; phosphorites; potassium fertilisers; beneficiation

Citation: Kalinina, N.; Maximov, P.; Makarov, B.; Dasi, E.; Rudmin, M. Characterisation and Environmental Significance of Glauconite from Mining Waste of the Egorievsk Phosphorite Deposit. *Minerals* **2023**, *13*, 1228. https://doi.org/10.3390/min13091228

Academic Editors: Pierre Giresse, Rachid Hakkou, Mohamed Loutou and Yassine Taha

Received: 10 August 2023
Revised: 7 September 2023
Accepted: 15 September 2023
Published: 19 September 2023

1. Introduction

Water soluble nitrogen, phosphorus and potassium are three essential elements that play an important role in plant growth and development [1]. Potassium plays an essential role in plant development. It promotes plant growth, participates in cellular homeostasis, contributes to charge balance, osmotic regulation and enzymatic catalysis, and provides immunity to disease [2–5]. Potash fertilisers are produced from sedimentary evaporite rocks such as sylvite, sylvinite and carnalite, as well as from surface and underground brines [6,7]. Many researchers are currently investigating the use of clay minerals [8–10], including glauconite, as potash slow-release or controlled-release fertilisers [2,4,6,7,11–14].

Glauconite is a dioctahedral, potassic, iron-rich clay mineral of predominantly marine origin [15–18]. Based on K_2O content, glauconite can be divided into four types: nascent (2%–4%), slightly evolved (4%–6%), evolved (6%–8%), and strongly evolved (>8%) [15,19]. The structure of glauconite consists of dioctahedral T–O–T sheets (tetrahedral–octahedral–tetrahedral). The octahedral sites usually contained more Fe^{3+} than Al^{3+} and significant amounts of Mg^{2+} and Fe^{2+}. Iron is mainly present in the form of Fe^{3+} in the glauconite structure [4,16]. Glauconite can absorb useful components [14,20,21] and be used as a complex fertiliser due to the special structure of the clay mineral [14,22].

The results of studies related to the use of glauconite as a sole source of potassium fertiliser have demonstrated positive effects on the growth of crops [11,13,23,24].

Glauconite is usually formed in a coastal-marine environment under conditions of sedimentary diagenesis [17,25]. Glauconite-rich beds occur in the sedimentary sequence with phosphorites [26–28] or, in some basins, with ironstones [11,29]. Glauconite rocks are potential secondary mineral products in sedimentary ironstone deposits [11]. However, glauconite from phosphorite deposits is poorly understood. Given the current knowledge on the various uses of glauconite in agriculture [2,4,6,7,11–14], ecology [30–33], the chemical industry [34,35], etc., it is necessary to pay attention to the evaluation of glauconite in mining wastes from phosphorite deposits under development. The positive prospects of glauconite from these deposits will contribute to the expansion of their raw material base and reduce the amount of mining waste at the expense of its use.

The aim of this work is to study the morphological, structural and chemical characteristics of glauconite from the waste of the Egorievsk phosphorite deposit in order to determine the potential for secondary use of mining waste in the agricultural sector.

2. Geological Background

The Egorievsk nodular phosphorite deposit is located 90 km southeast of Moscow and covers an area of about 950 km^2 [36,37]. Tectonically, the field is confined to a depression on the East European Platform, enclosed between the Oka-Tsninsk rampart and the Voronezh anteclise. The area consists of Middle and Upper Jurassic and Lower Cretaceous sedimentary rocks deposited on the eroded surface of Carboniferous limestone (Figure 1).

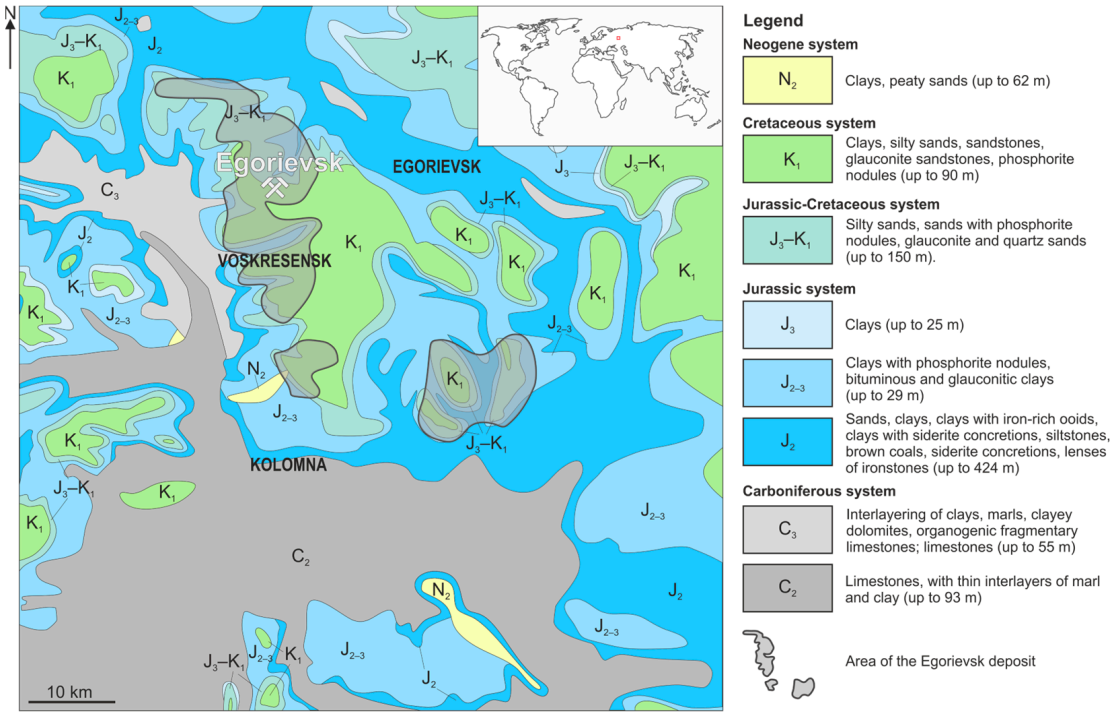

Figure 1. Scheme of the geological structure of the southeastern part of Moscow region with the location of the Egorievsk deposit according to [38].

The rocks lie monoclinic with a slight dip of layers to the northeast [37].

The ores from the Egorievsk deposit belong to the group of glauconite phosphorites and are characterised by complex compositions [38]. They consist of phosphate (45%), glauconite (25%–30%), and quartz (25%). Phosphate minerals are represented by fluorapatite and carbanapatite (kurskite) [39,40]. The ores also contain feldspars, pyrite, calcite, and iron hydroxides [40].

The productive phosphorite series includes rocks of the Volga stage of the Upper Jurassic and the Ryazan horizon of the Lower Cretaceous. It includes the lower and

upper phosphorite layers (horizons), separated by a pack of quartz-glauconite sands (Figure 2) [37].

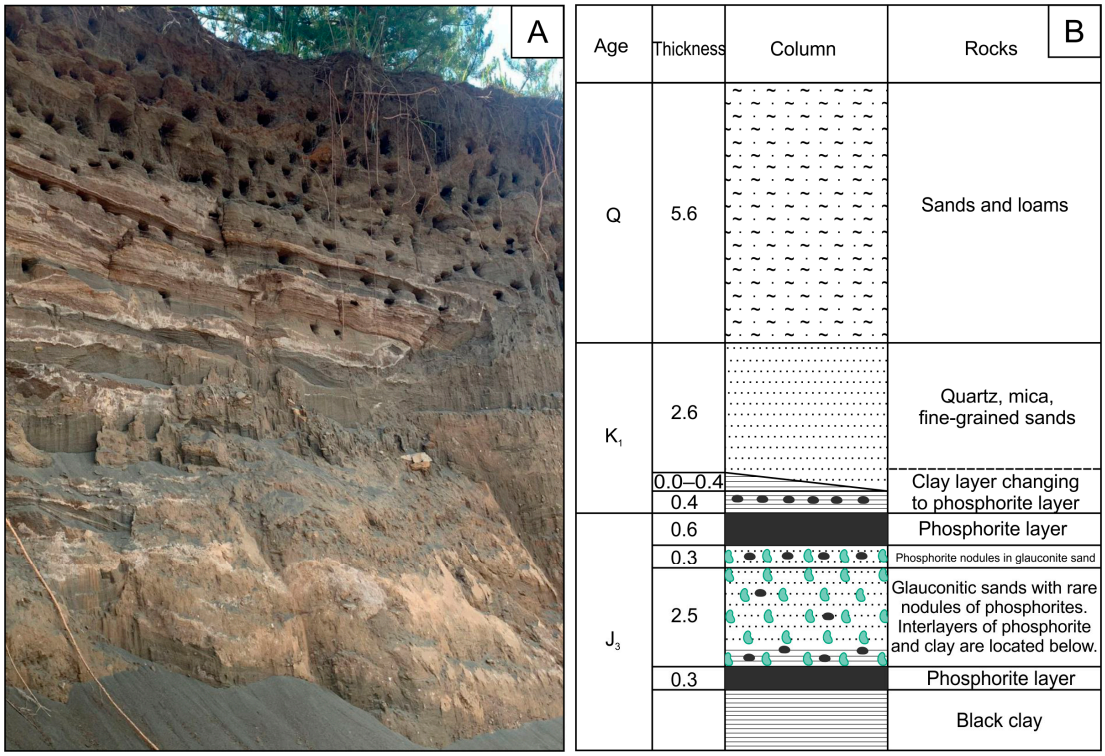

Figure 2. (**A**) Photo of the sampling site; (**B**) lithological section of phosphorite of the Egorievsk deposit [37].

Phosphorite layers are represented by nodular phosphorites and phosphatised ammonites in clayey and sandy sediments. The nodules are composed of phosphates with silty intrusions of quartz, glauconite, feldspar, less frequently hydromica and pyrite. The content of glauconite in the layers reaches 30%–33%. The thickness of the phosphorite layers ranges from the first tens of centimetres to 1.5 m. The quartz–glauconite sandstones separating the two phosphorite layers are composed of fluorocarbonapatite (up to 15%), glauconite (up to 49%), hydromica (up to 15%) and quartz (up to 11%) [37,39]. The thickness of the quartz–glauconite sequence varies between 0.13 and 7.8 m, with an average thickness of 2 m. Quartz–glauconite sands contain layers and lenses of glauconite clay with occasional sandy-type phosphoric nodules [37].

Phosphorites were deposited under reducing conditions in shallow marine basins with limited input of terrigenous material from the continent. Phosphorite layers contain benthic fauna, mainly sponge remains, and diverse organisms, including nektonic and planktonic species. The formation of phosphorite concretions from amorphous phosphate occurred in marine mud at a depth of about 100 metres. The formation of phosphorites is characterised by a sequential process involving: 1. accumulation of clastic minerals and organic remains; 2. development of globular glauconite; 3. formation of concretions of amorphous phosphate; 4. crystallisation of radially fibrous phosphate within phosphorite pores; 5. precipitation of pyrite and leaching of amorphous silica [36].

At the former mining and processing plant, which processed phosphorite ores from the Egorievsk deposit, only selectively mined phosphorites from the upper and lower layers were enriched, but glauconite sands were sent to landfills or for reclamation of disturbed lands [39]. The primary enrichment of the phosphate rock was carried out by the gravity method. Water served as a flushing fluid to separate the phosphate concentrate. After the beneficiation process, large dumps rich in glauconite are formed. This study focuses on the glauconite waste from the Egorievsk deposit.

3. Materials and Methods

The material used for the study was loose waste from the Egorievsk deposit, which has a high glauconite content. A magnetic concentrate with a higher glauconite content was obtained by electromagnetic separation of the initial mining waste samples. The separation was carried out using an EVS-10/5 (NPK Mekhanobr-Technika, Saint- Petersburg, Russia). Glauconite concentrate weighing 230 g was producing from 500 g of bulk sample. Five glauconite concentrate samples and three bulk samples were selected for laboratory analyses. The samples used for the study were loose samples, powdered samples, checkers and tablets.

Laboratory analyses used to investigate bulk waste and glauconite concentrate samples include the following analytical methods: X-ray diffraction analysis (XRD), scanning electron microscopy (SEM), transmission electron microscopy (TEM), X-ray fluorescence analysis (XRF), infrared spectrometry (FTIR), and inductively coupled plasma mass spectrometry (ICP-MS).

X-ray diffraction analysis was carried out to investigate the bulk mineral composition of the concentrate and to identify clay minerals. For analysis, the samples were dried, crushed in a roll crusher and then ground in a mill to a powder (powder, particle size not exceeding 10 μm). The clay fraction (less than 2 microns) of all samples was obtained by successive procedures: crushing, dispersion of the debris in an ultrasonic bath, preparation of a suspension, removal of the terrigenous part (quartz, feldspars). The suspension was then left to stand in a column of distilled water for 8 to 16 h (according to Stokes' law and the operator's estimate of the sedimentation rate of the particles), the top of the suspension was broken off in a centrifuge (3000 rpm) and sent for analysis. The images were recorded on a Rigaku Ultima IV with a Cu Kα anode at 40 kV and 30 mA. Imaging was performed over a range of 3–65° on the 2-theta scale at a rate of 1° per minute in 0.02° increments. The clay fraction was taken dry, saturated with organic liquid (ethylene glycol) and after heating/roasting at 550 °C to identify phyllosilicates. In general, all procedures were carried out according to generally accepted recommendations [41]. Quantification was performed using the Rietveld method [42] with PDXL and Siroquant software (version 5) using the PDF-2, PDF-4 and PDF-14 databases (ICDD, Denver, CO, USA). Data on glauconite were obtained from the PDF 2014 database, card PDF 00-063-0583. The average measure of inaccuracy of the method was 1%. The accessory minerals were not included in the calculations and probably account for a bulk fraction of less than 0.5%.

Scanning electron microscopy was carried out on a loose sample and a checkerboard to determine the mineral composition of the bulk sample and concentrate and to study the morphology and chemical composition of glauconite. SEM was performed using a TESCAN VEGA 3 SBU microscope (Teskan, Brno, Czech Republic) equipped with an OXFORD X-Max 50 (Oxford Instruments, Abingdon, United Kingdom) energy dispersive detector. The accelerating voltage (hv) for SEM imaging and analysis was 20 kV with the probe current intensity ranging from 4.5–11.5 nA.

Transmission electron microscopy was used to determine the mineral composition of the globules and the structure of glauconite. PEM was carried out using a JEOL JEM-2100F (JEOL, Tokyo, Japan) transmission electron microscope. A drop of the clay suspension was dried on a copper mesh (300 meshes, 3.05 mm diameter) before being examined by TEM at an accelerating voltage of 200 kV.

X-ray fluorescence analysis was performed to compare the geochemical characteristics of the bulk sample and the concentrate. Concentrations of basic oxides (Fe_2O_3, SiO_2, Al_2O_3, Na_2O, MgO, P_2O_5, K_2O, CaO, TiO_2, MnO) were determined using an X-ray fluorescence microanalyzer HORIBA XGT 7200 (HORIBA Ltd., Moscow, Russia). Special samples (pressed pellets) of finely ground mass were prepared for the research. Powdered samples were pressed under a hydraulic press, after which they were baked in a muffle furnace at 900 °C for 9 h with an assessment of the loss on ignition as the difference in weight before and after baking.

Infrared spectroscopy was employed to determine the functional groups present in the chemical bonding of glauconite, as well as to identify microinclusions. Infrared spectra of the composites were obtained in the range of 4000–400 1/cm using an FTIR spectrometer (Shimadzu FTIR 8400S, Kyoto, Japan) with a temperature-controlled high-sensitivity detector (DLATGS) of KBr tablets with a resolution of 4 1/cm.

Inductively coupled plasma mass spectrometry (ICP-MS) was performed to determine heavy metal contents in glauconite concentrate and the bulk glauconite rock. The investigation was carried out using an ELAN DRC mass spectrometer. The analytical sample with a mass of approximately 0.5 g was subjected to melting at 1050 °C for 15 min. A $LiBO_2/Li_2B_4O_7$ mixture was used as a fluxing agent to ensure optimal melting conditions. This process produced glassy beads which were then dissolved in a mixture of HF, HNO_3 and $HClO_4$ acids in a ratio of 5:4:1.5 at 120 °C. The dissolution was carried out in a platinum crucible for 6 h to ensure complete decomposition of the samples. The liquid extract obtained was evaporated at 160 °C. After evaporation, the sample residue was dissolved in 10 mL of 5 M HNO_3 solution. The solution was then filtered to remove particles and precipitates and sent for analysis.

Laboratory experiments were carried out on the cultivation of agricultural crops with the addition of a bulk sample and glauconite concentrate. Soil without fertiliser was used as control and rationing cells. Oat (*Avéna satíva*) seeds were grown in glass Petri dishes (9 cm diameter, 1.5 cm depth) at room temperature (26 ± 1 °C) for 20 days. Dry samples of glauconite rock and glauconite concentrate were applied to the soil at a rate of 90 kg per hectare. Each experiment was replicated three times (cell) and averaged. A slightly acidic, dark grey agricultural soil (pH 5.1) with 4.1% organic carbon was used for the experiments. Plants were watered every morning with tap water. Germination energy, germination rate, plant height and dry weight of the plants were determined [11,43]. Germination was estimated as the ratio of the number of sprouts to the number of seeds sown. Germination energy was recorded daily, and the final percentage of germination was determined after 4 days. The number of shoots was determined assuming that the plants were 2 cm above the soil surface. Height and weight of plants were measured after 20 days. Oat seedlings were individually wrapped in a paper sheet and stored in a desiccator at 80 °C. The dry weight of the plants was measured when the weight of the samples had stabilised.

Statistical analysis of the results was performed using the program Microsoft Excel 365. Values were calculated as arithmetic mean with standard deviations. The average values were determined by the least significant difference (LSD) test at the 0.05 probability level. Analysis of variance, followed by LSD and one-way ANOVA were used to determine significant differences between experiments and among treatments, respectively.

4. Results

4.1. Research and Enrichment of Glauconite from Waste of the Egorievsk Deposit

4.1.1. Characteristics of Mining Waste from the Deposit and Enrichment of Glauconite Concentrate

The waste from the Egorievsk deposit consists of glauconite (42.2%), apatite, quartz, pyrite, gypsum, goethite and ilmenite. In order to obtain the concentrate with the maximum content of globular glauconite, the following parameters of electromagnetic separation were chosen: current—7A, distance from the feed to the path—2 mm, distance from the shaft to the path—4 mm, and average speed—2.5 cm/s. The glauconite content increased twofold as a result of the enrichment of the bulk sample (86.1%, Figure 3).

In addition to glauconite, kaolinite and smectite (Figure 4), as well as apatite (Figure 4), pyrite, and goethite are observed in the concentrate.

The pyrite content in the concentrate does not exceed 5%. According to the XRF data (Table 1) in the bulk composition of the concentrate there is an increase in elements included in the glauconite composition (K_2O, Fe_2O_3) and a decrease in elements characteristic to quartz, apatite and gypsum (SiO_2, P_2O_5, CaO), which confirms the increase in glauconite concentration in the concentrate.

Table 1. Chemical composition (%) of bulk sample and glauconite concentrate of the Egorievsk deposit.

	Na_2O	MgO	Al_2O_3	SiO_2	P_2O_5	K_2O	CaO	TiO_2	MnO	Fe_2O_3	SUMM	LOI
BS	0.8	1.3	11.1	43.6	6.2	2.9	6.9	0.2	0.1	11.1	84.2	15.8
GC	0.4	1.3	9.5	41.5	2.0	5.0	2.7	0.3	0.1	28.9	91.4	8.6

Note: BS—bulk sample, GC—glauconite concentrate.

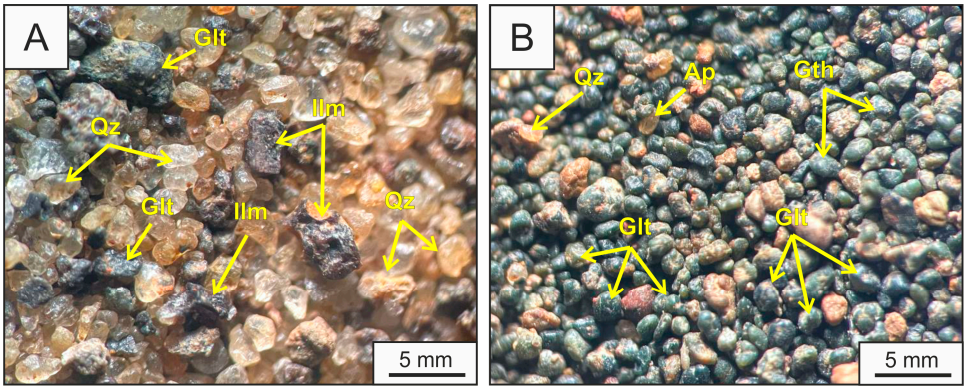

Figure 3. Photos of the bulk sample (**A**) and glauconite concentrate (**B**) obtained by electromagnetic separation under a binocular microscope. Ap—apatite, Glt—glauconite, Gth—goethite, Ilm—ilmenite, Qz—quartz.

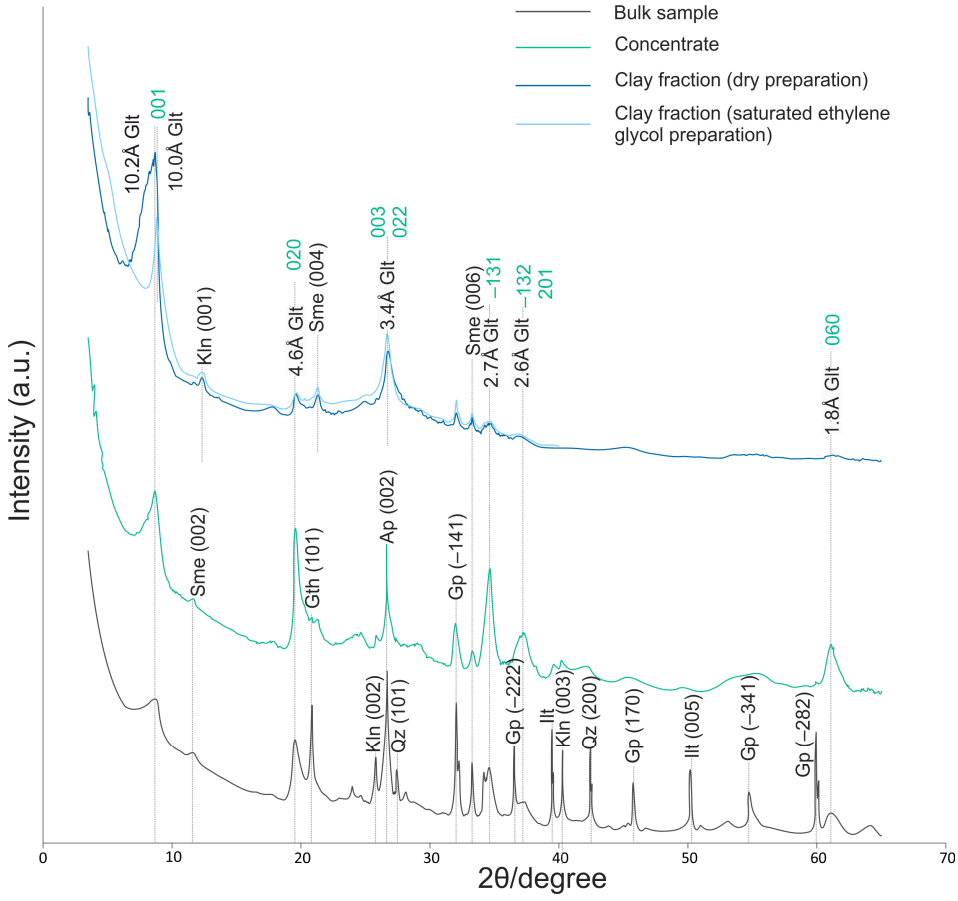

Figure 4. Diffractograms of bulk sample, glauconite concentrate and clay fraction. Ap—apatite, Glt—glauconite, Gp—gypsum, Gth—goethite, Ilt—illite, Kln—kaolinite, Qz—quartz, Sme—smectite.

4.1.2. Mineralogical and Geochemical Features of Glauconite

Glauconite has a globular shape of grains ranging in size from 60 to 370 µm (Figure 5A–C). Globules are composed of chaotically arranged flaky crystals up to 0.25 µm in size (Figures 5D and 6).

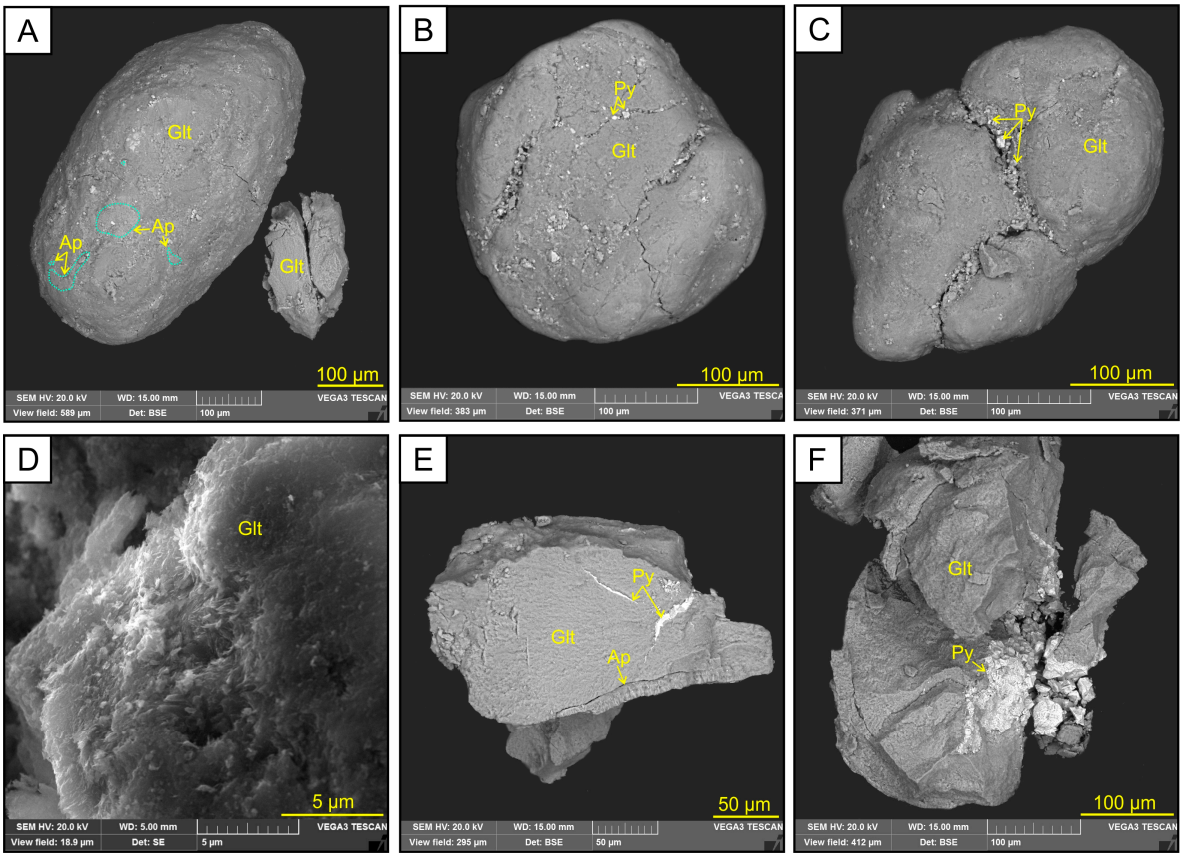

Figure 5. Electronic images: (**A**–**C**) globular glauconite with inclusions of apatite (**A**) and pyrite (**B**,**C**); (**D**) chaotically oriented glauconite flakes; (**E**) fragment of glauconite grain with sparry apatite aggregate and pyrite veins; (**F**) split glauconite grain with pyrite inclusion. Ap—apatite, Glt—glauconite, Py—pyrite.

X-ray diffractograms of glauconite show the following main basal reflexes: 10.2 and 3.4 Å. The hkl reflexes are additionally reflected in the 4.6 Å (020), 3.4 Å (003; 022), 2.7 Å (−131), 2.6 Å (−132; 201) and 1.8 Å (060). The maximum reflex of 10.2 Å (001) is slightly asymmetric and shifts to 10.00 Å after ethylene glycol impregnation. In addition to glauconite, basal reflexes of apatite, gypsum, goethite, quartz, illite and kaolinite are present. The intensity of the basal reflexes of diamagnetic minerals (apatite, gypsum, quartz) decreased after magnetic separation. The decrease in intensity of diamagnetic minerals indicates a decrease in their content in the concentrate.

In the electron diffraction patterns, glauconite is characterised by peaks at 10.9, 4.8, 3.1, 2.6, 1.6 Å, and apatite—8.4, 4.3, 2.8, 1.9 Å (Figure 6B,C). The width of the T–O–T layers is 7.6–7.9 Å (Figure 6D). Chemical composition of the original glauconite according to SEM EDS analysis is as follows: K_2O 6.1%–9.0%, $Fe_2O_{3(total)}$ 16.2%–26.9%, SiO_2 48.0%–51.9%, Al_2O_3 5.3%–14.5%, MgO 2.0%–3.0%, CaO 0.6%–2.4%. In addition, glauconite has good sorption capacity and contains a number of heavy metals that can have negative effects on plants and contaminate soil. (Table 2).

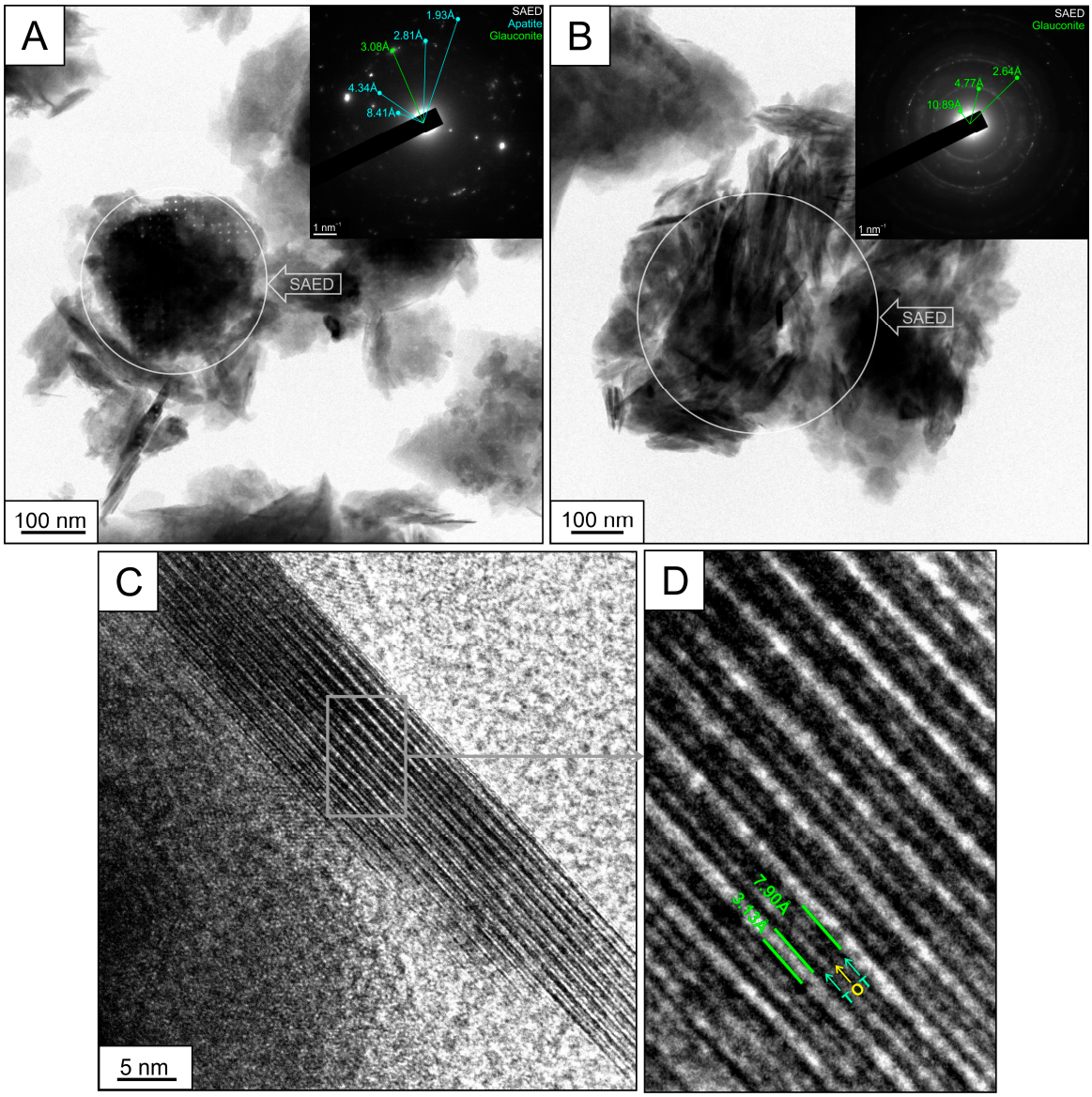

Figure 6. TEM-images of glauconite and local electron diffraction patterns: (**A**) apatite grain surrounded by glauconite flakes, (**B**,**C**) glauconite flake crystals, (**D**) glauconite crystal structure showing dioctahedral sheets (T–O–T).

Table 2. Contents of heavy metals in bulk sample and glauconite concentrate according to ICP-MS data and limit allowable concentrations of heavy metals in different regions.

	BS	GC	Texas [44]	Brazil [45]	Europe [45]	USA [45]	Russia [46]
Cr	26.9	45.0		200	56	55	
Ni	32.7	66.8	420	70	44		100
Cu		5.3			60	172	600
Zn	131.8	227.5	370		347	556	1500
As	11.9	15.7	41				20
Se	6.4	8.4	100				
Mo	0.8	1.1	18				
Cd	0.1	0.2	39	3	0.7	0.8	20
Pb	8.5	7.9	300	150	18	27	120

Note: BS—bulk sample, GC—glauconite concentrate.

A detailed analysis of the mineral composition of globules often shows fluorapatite (Figures 5A,E and 6A,B), less common are pyrite (Figure 5B,C,E,F) and goethite (Figure 7). Fluorapatite occurs as small, xenomorphic grains (Figure 6A,B), bound by flaky glauconite crystals. The proportion of fluorapatite in some globules reaches 50%. The content of fluorine in apatite is 3.0%–8.9%. Fluorapatite is also detected on the infrared spectrum (Figure 7). The presence of microinclusions of apatite is indicated by peak characterising (PO_4^{3-}) at 602 1/cm. Pyrite occurs as grains or fine crystalline aggregates (Figure 5C,E,F), filling voids and fissures in glauconite globules. Pyrite is often partially or completely replaced by goethite.

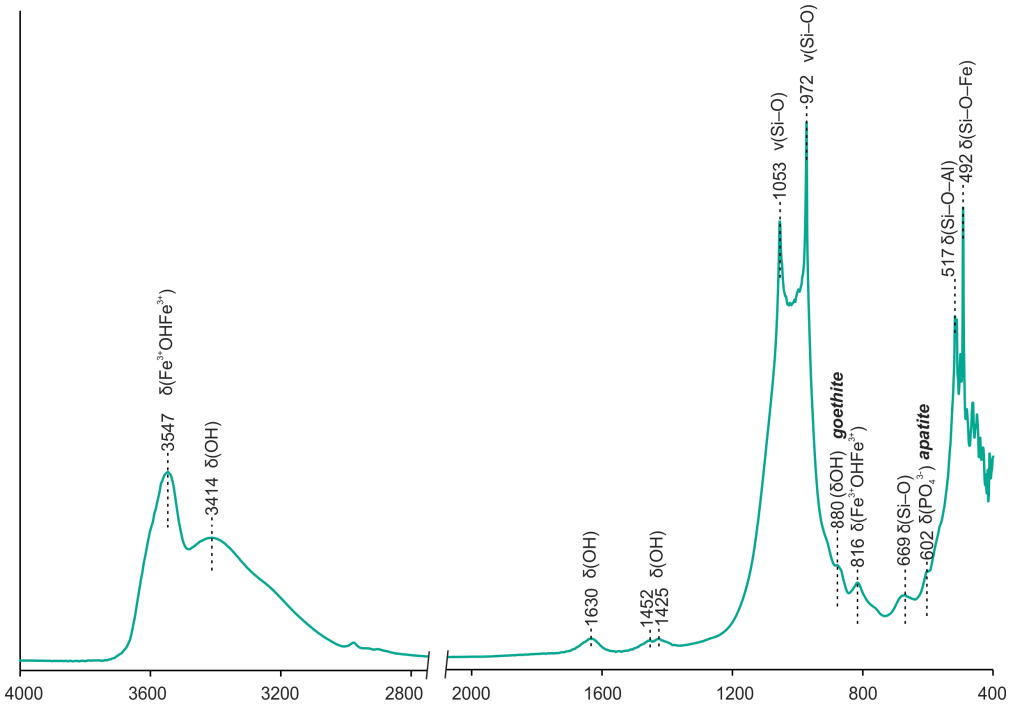

Figure 7. FTIR-spectrum of glauconite from mining waste.

The strain and symmetric (valence) vibration zone is characterised by peaks 1053–972 and 669 1/cm corresponding to ν(Si-O) and δ(Si-O), according to infrared spectrometry of glauconite. The oscillation peak at 816 1/cm indicates the presence of hydroxyl with trivalent iron ($Fe^{3+}OHFe^{3+}$) in the octahedral position. The peak characterising the strain variations of Al (AlOHAl) is usually found in the region at 912–914 1/cm. However, the peak is shifted and represented by ($AlOHFe^{3+}$) at 880 1/cm, probably due to microinclusions of goethite. In the high frequency region of the octahedral position, peaks 3547 and 3414 corresponding to $Fe^{3+}OHFe^{3+}$ and OH.

4.2. Investigation of Glauconite Application in Laboratory Conditions

The germination energy (e.g., *Avéna satíva* oat was used) with glauconite rock and glauconite concentrate was 94.7%–96.0% (Figure 8A), which is higher than in the control cell without fertiliser (92.7%). The peak of this figure was obtained with an unenriched sample.

The germination rate of the plants in the test cells ranged from 94.9% to 96% (Figure 8B), exceeding the control germination level (94.1%). The highest percentage of germination was achieved with the glauconite concentrate.

Average plant height varied between 12.5 and 12.7 cm when the test fertilisers were used (Figure 8C), compared with the control value of 11.9 cm. This represents an increase in plant growth of 5.6 and 6.7% when using glauconite rock and glauconite concentrate, respectively.

There was also an increase in plant dry weight (yield) in all treatments, compared to the control. The dry weight of the plants ranged from 0.21 to 0.22 g (Figure 8D), while the

control dry weight was 0.20 g. As a result, the yield in the cells with glauconite rock and glauconite concentrate increased by 3.5% and 6.3%, respectively.

The results of a series of laboratory experiments showed that the glauconite concentrate had the most significant stimulating effect on plant growth and development. At the same time, a stable positive effect was also demonstrated using an untreated mining waste sample.

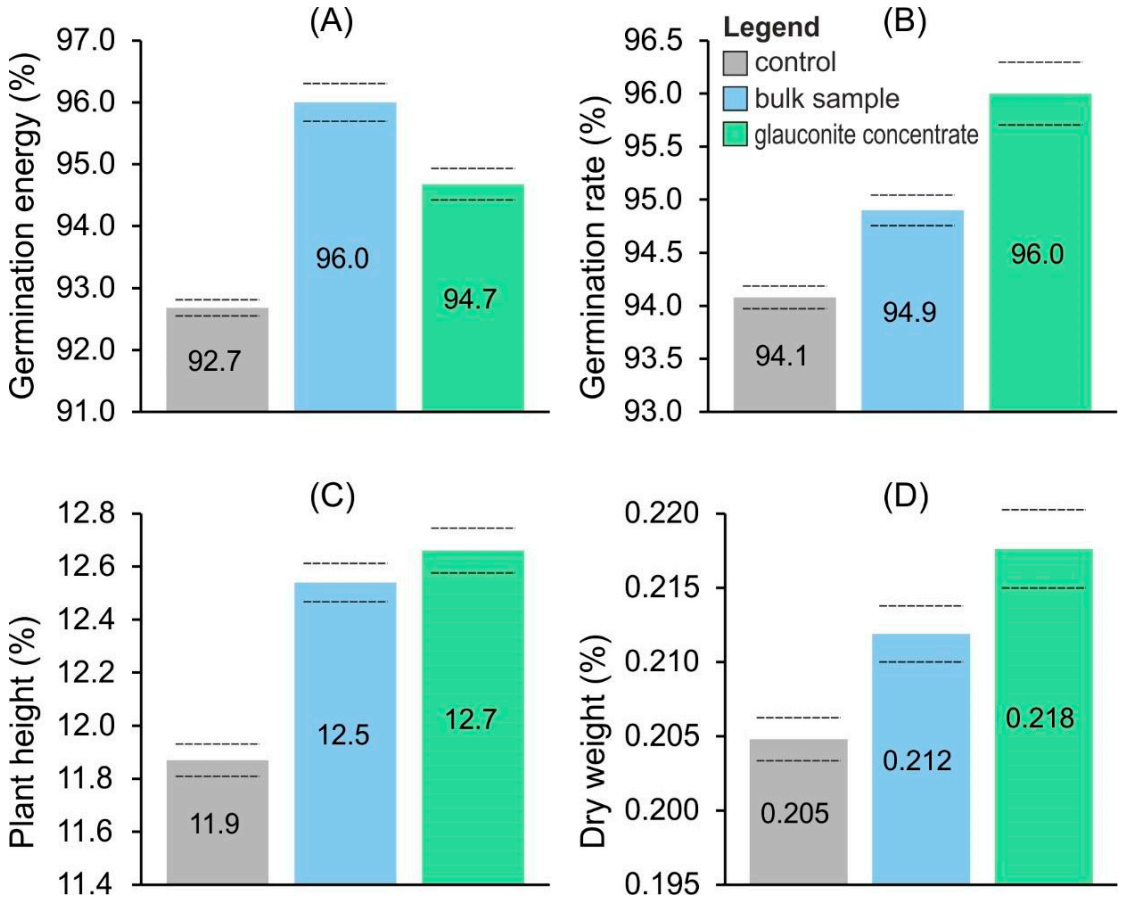

Figure 8. Histograms of the distribution of the main growth parameters of common oat (*Avéna satíva*) using glauconite rock and glauconite concentrate: (**A**) germination energy, (**B**) germination, (**C**) plant length, and (**D**) dry weight or yield. The statistical significance of each parameter is shown at $p = 0.05$. The dotted lines show the standard deviation of the parameter.

5. Discussion

5.1. Mining Waste Enrichment

The waste resulting from phosphate rock enrichment comprises a variety of minerals, including glauconite. An electromagnetic separation method was utilised to extract a concentrate of glauconite. This enrichment process resulted in a twofold rise of the glauconite concentration in the final product and consequently in the potassium content (Table 1).

5.2. Morphology and Chemical Composition of Glauconite: Key Factors Determining Usefulness in the Agricultural Sector

Glauconite is present in the shape of spherical grains (Figure 5). According to SEM-EDS information, the crystallochemical composition can be expressed as: $K_{0.5\text{-}0.7}Ca_{0\text{-}0.2}(Al_{0\text{-}0.4}Mg_{0.2\text{-}0.3}Fe_{0.8\text{-}1.3})_{1.0\text{-}2.0}(Si_{2.9\text{-}3.5}Al_{0.5\text{-}1.0})O_{10}(OH)_2nH_2O$. According to the classification by G. Odin, glauconite obtained from the waste of the Egorievsk deposit belongs to the "evolved" varieties [15]. This is attributed to its high potassium content, ranging from 6 to 9%. Furthermore, glauconites from this deposit exhibit the first basal reflection 001 at 10 Å

(Figure 4), which is a distinguishing feature of mature glauconites, as opposed to nascent glauconites, where the reflection can be found at 14 Å [15].

The chemical composition and morphology of glauconite render it an effective fertiliser. The potassium in glauconite is critical in regulating the plant's water balance and the process of photosynthesis [2–5]. The presence of magnesium and iron in glauconite also aids in increasing the photosynthetic activity of plants [47–50]. In addition, it is essential to highlight that glauconite serves as both a valuable fertiliser and a crucial component for enhancing agronomic features of soil, which in turn increases agricultural productivity. It has the ability to preserve moisture and ensure favourable soil aeration, thereby promoting the growth of plant roots [11,13]. This holds particular significance in areas with restricted water resources or during arid climatic conditions. The favourable globular shape and crumbly nature of the waste facilitates its separation and incorporation into the soil, making it very practical and convenient for use in agriculture.

Despite the advantages of glauconite for plant growth, it is crucial to consider the potential risks linked to its application. Being a type of clay mineral, glauconite exhibits a high capacity for sorption, resulting in the accumulation of various toxic elements in its composition. The Egorievsk deposit shows that their concentrations remain at low levels [51–53], which makes it possible to use these rocks as fertilisers. Phosphate meal produced from phosphate rock at the Egorievsk deposit has been successfully used as fertiliser. The use of waste from phosphate rock processing as a fertiliser will allow efficient use of production waste. According to ICP-MS data (Table 2), the content of heavy metals is below the permissible limit both in the wastes of the Egorievsk deposit and in the concentrate obtained from the wastes.

5.3. Microinclusions in Glauconite and Their Role for Plants

Apatite and pyrite are often found as part of glauconite globules (Figures 5, 6A and 7). Pyrite, which is present in glauconite grains, is not harmful to plants and may even be beneficial. Modern research considers pyrite to be one of the components of fertilisers because it increases the availability of sulphur in the soil and the easy absorption of other useful trace elements by plants [54–56]. Apatite, a component of glauconite, can also have a positive effect. In acidic soils (pH 2–7), apatite can dissolve, partially releasing phosphorus for plants [57,58]. In addition, the phosphorus released may interact with heavy metals in the soil or those accumulated by the glauconite. This limits the solubility and bioavailability of heavy metals to plants [58] and reduces the negative impact of these metals on plants and the ecosystem as a whole. Glauconite fertilisers with apatite can therefore provide a valuable means of improving soil fertility while reducing potential environmental damage.

Applying apatite to acidic soils can also increase the alkalinity (raise the pH) of the soil [59]. This process can be positive if the soil is initially acidic and requires neutralisation to provide more favourable conditions for plant growth. Agrotests to evaluate the effectiveness of glauconite fertilisers were conducted on slightly acidic soils and showed significantly positive results. This confirms the prospect of using glauconite from the Egorievsk deposit on soils characterised by low pH.

5.4. Agrotests

The investigation of the effects of glauconite waste and glauconite concentrate on plant growth, in this case on the model crop oat (*Avéna satíva*), led to the identification of significant advantages of these fertilisers. Through laboratory experiments, it was demonstrated that glauconite concentrate had the greatest stimulating effect on plant growth and development (Figure 8). However, it is important to note that a consistent positive effect was also observed when utilising untreated samples of mining waste. The most notable indices are seen in germination energy and germination rate, demonstrating the potential of the investigated glauconite to promote successful seed germination and vigorous plant growth from the point of sprouting.

During the experiment, the researchers analysed acidic soils, and the study's findings confirmed the effectiveness of using glauconite fertilisers for these soil types. Given the composition of the concentrate and the presence of apatite within it, which aids in raising soil pH levels, it is recommended to consider glauconite fertilisers as a promising solution to rectify acidic soils and increase their fertility.

The agrotest results suggest that glauconite fertilisers have the potential to raise crop yields. The increase in plant dry weight and the active formation of seedlings confirm the effectiveness of using waste from the Egorievsk deposit in the agricultural sector.

6. Conclusions

As a result of the investigation of glauconite-containing rocks from the mining waste of the phosphorite deposit, the following conclusions were obtained.

(1) Concentrating glauconite among the loose waste contributes to the economically available enrichment of the mineral concentrate by means of electromagnetic separation with the fraction of the useful component being 86%.
(2) Morphological and structural–chemical features of the glauconite allow it to be referred to as a mature, rather discrete variety. The proportion of ion exchangeable potassium up to 9% and the favourable globular shape of the grains indicate the potential use of glauconite from mining waste as a mineral fertiliser.
(3) The presence of apatite and pyrite inclusions in glauconite significantly increases the value of the fertiliser. Pyrite makes sulphur available to plants, while apatite releases phosphorus in acidic soils and reduces the risk of heavy metal contamination. These factors make this fertiliser more effective and environmentally safe.
(4) Glauconite rocks and glauconite concentrate demonstrated a positive effect on plant growth and development in laboratory experiments. The yield of common oats (Avena sativa) increased by 3.5% and 6.3% when glauconite-containing rocks and glauconite concentrate from the mining waste of the phosphorite deposit were used, respectively.
(5) Egorievsk waste fertiliser can be most beneficial when used on acidic soils and in regions with limited moisture.

Waste from phosphate rock processing at the Egorievsk deposit is a valuable source of glauconite for fertiliser production. Its use allows us to make efficient use of production waste and enrich the raw material base for fertiliser production.

Author Contributions: Conceptualization, M.R.; methodology, M.R., N.K. and B.M.; validation, N.K., P.M. and B.M.; formal analysis, N.K., P.M. and B.M.; investigation, M.R., N.K., P.M. and B.M.; resources, M.R.; data curation, M.R.; writing—original draft preparation, N.K., P.M., E.D. and M.R.; writing—review and editing, N.K. and M.R.; visualization, N.K.; supervision, M.R.; project administration, M.R.; funding acquisition, M.R. All authors have read and agreed to the published version of the manuscript.

Funding: This research was funded by Russian Science Foundation through the research project No. 22-77-10002.

Data Availability Statement: Data is contained within the article.

Acknowledgments: N.K. acknowledges support project FSWW-2023-0010. Authors are thankful to two anonymous reviewers and the editor for their valuable comments and constructive reviews of earlier versions of this paper.

Conflicts of Interest: The authors declare no conflict of interest.

References

1. Falls, J.H.; Siegel, S.A.; Industries, C.F.; City, P. *Fertilisers Types of Fertilizer Materials Analytical Methods for Nitrogen*; Elsevier: Amsterdam, The Netherlands, 2013. [CrossRef]
2. Rakesh, S.; Juttu, R.; Bairi, R. Glauconite: An Indigenous and Alternative Source of Potassium Fertilizer for Sustainable Agriculture. *Int. J. Bioresour. Sci.* **2020**, *7*, 17–19. [CrossRef]

3. Zörb, C.; Senbayram, M.; Peiter, E. Potassium in agriculture—Status and perspectives. *J. Plant Physiol.* **2014**, *171*, 656–669. [CrossRef] [PubMed]
4. Shekhar, S.; Sinha, S.; Mishra, D.; Agrawal, A.; Sahu, K.K. A sustainable process for recovery of potash fertilizer from glauconite through simultaneous production of pigment grade red oxide. *Sustain. Mater. Technol.* **2020**, *23*, e00129. [CrossRef]
5. Manning, D.A.C. Mineral sources of potassium for plant nutrition. A review to cite this version: Mineral sources of potassium for plant nutrition. A review. *Agron. Sustain. Dev.* **2010**, *30*, 281–294. [CrossRef]
6. Santos, W.O.; Mattiello, E.M.; Marciano, L.; Antônio, W.; Abrahão, P.; De Novais, R.F.; Cantarutti, R.B. Thermal and chemical solubilization of verdete for use as potassium fertilizer. *Int. J. Miner. Process.* **2015**, *140*, 72–78. [CrossRef]
7. Shekhar, S.; Mishra, D.; Agrawal, A.; Sahu, K.K. Physical and chemical characterization and recovery of potash fertilizer from glauconitic clay for agricultural application. *Appl. Clay Sci.* **2017**, *143*, 50–56. [CrossRef]
8. Borges, R.; Brunatto, S.F.; Leitão, A.A.; De Carvalho, G.S.G.; Wypych, F. Solid-state mechanochemical activation of clay minerals and soluble phosphate mixtures to obtain slow-release fertilisers. *Clay Miner.* **2015**, *50*, 153–162. [CrossRef]
9. Borges, R.; Prevot, V.; Forano, C.; Wypych, F. Design and Kinetic Study of Sustainable Potential Slow-Release Fertilizer Obtained by Mechanochemical Activation of Clay Minerals and Potassium Monohydrogen Phosphate. *Ind. Eng. Chem. Res.* **2017**, *56*, 708–716. [CrossRef]
10. Lei, Z.; Cagnetta, G.; Li, X.; Qu, J.; Li, Z.; Zhang, Q.; Huang, J. Enhanced adsorption of potassium nitrate with potassium cation on H3PO4 modified kaolinite and nitrate anion into Mg-Al layered double hydroxide. *Appl. Clay Sci.* **2018**, *154*, 10–16. [CrossRef]
11. Rudmin, M.; Banerjee, S.; Mazurov, A.; Makarov, B.; Martemyanov, D. Economic potential of glauconitic rocks in Bakchar deposit (S-E Western Siberia) for alternate potash fertilizer. *Appl. Clay Sci.* **2017**, *150*, 225–233. [CrossRef]
12. Rudmin, M.; Oskina, Y.; Banerjee, S.; Mazurov, A.; Soktoev, B.; Shaldybin, M. Roasting-leaching experiments on glauconitic rocks of Bakchar ironstone deposit (Western Siberia) for evaluation their fertilizer potential. *Appl. Clay Sci.* **2018**, *162*, 121–128. [CrossRef]
13. Rudmin, M.; Banerjee, S.; Makarov, B.; Mazurov, A.; Ruban, A.; Oskina, Y.; Tolkachev, O.; Buyakov, A.; Shaldybin, M. An investigation of plant growth by the addition of glauconitic fertilizer. *Appl. Clay Sci.* **2019**, *180*, 105178. [CrossRef]
14. Rudmin, M.; Banerjee, S.; Yakich, T.; Tabakaev, R.; Ibraeva, K.; Buyakov, A.; Soktoev, B.; Ruban, A. Formulation of a slow-release fertilizer by mechanical activation of smectite/glauconite and urea mixtures. *Appl. Clay Sci.* **2020**, *196*, 105775. [CrossRef]
15. Odin, G.S.; Matter, A. De glauconiarum origine. *Sedimentology* **1981**, *28*, 611–641. [CrossRef]
16. Dooley, J.H. Glauconite. In *Industrial Minerals and Rocks: Commodities Market and Uses*; Koger, J., Trivedi, N., Barrer, J., Krukowsky, N., Eds.; Society for Mining, Metallurgy and Exploration: Littleton, CO, USA, 2006; pp. 493–495.
17. Banerjee, S.; Bansal, U.; Vilas Thorat, A. A review on palaeogeographic implications and temporal variation in glaucony composition. *J. Palaeogeogr.* **2016**, *5*, 43–71. [CrossRef]
18. Banerjee, S.; Bansal, U.; Pande, K.; Meena, S.S. Compositional variability of glauconites within the Upper Cretaceous Karai Shale Formation, Cauvery Basin, India: Implications for evaluation of stratigraphic condensation. *Sediment. Geol.* **2016**, *331*, 12–29. [CrossRef]
19. Amorosi, A. Detecting compositional, spatial, and temporal attributes of glaucony: A tool for provenance research. *Sediment. Geol.* **1997**, *109*, 135–153. [CrossRef]
20. Sing, S.; Bhadauria, R.; Tomar, R. Sorption of Cd^{2+}, Hg^{2+} and Pb^{2+} by synthetic analogue of mica mineral glauconitic. *J. Appl. Chem.* **2010**, *6*, 287–295.
21. Smith, E.H.; Lu, W.; Vengris, T.; Binkiene, R. Sorption of heavy metals by Lithuanian glauconite. *Water Res.* **1996**, *30*, 2883–2892. [CrossRef]
22. Terentyev, Y.N.; Syrchina, N.V.; Bogatyryova, N.N.; Ashikhmina, T.Y.; Sazanov, A.V.; Sazanova, M.L.; Pugach, V.N.; Kozvonin, V.A.; Burkov, A.A. The use of glauconite for stabilization and improvement of ammonium nitrate agrochemical properties. *Theor. Appl. Ecol.* **2018**, *2018*, 61–67. [CrossRef]
23. Karimi, E.; Abdolzadeh, A.; Sadeghipour, H.R.; Aminei, A. The potential of glauconitic sandstone as a potassium fertilizer for olive plants. *Arch. Agron. Soil Sci.* **2012**, *58*, 983–993. [CrossRef]
24. dos Santos Torqueti, S.T.; Boldrin, K.V.F.; do Nascimento, Â.M.P.; de Oliveira Paiva, P.D.; Furtini Neto, A.E.; Luz, I.C.A. Fonte alternativa de potássio no cultivo do girassol ornamental. *Agric. Sci.* **2016**, *40*, 257–264. [CrossRef]
25. Chafetz, H.S.; Reid, A. Syndepositional shallow-water precipitation of glauconitic minerals. *Sediment. Geol.* **2000**, *136*, 29–42. [CrossRef]
26. Banerjee, S.; Farouk, S.; Nagm, E.; Choudhury, T.R.; Meena, S.S. High Mg-glauconite in the Campanian Duwi Formation of Abu Tartur Plateau, Egypt and its implications. *J. Afr. Earth Sci.* **2019**, *156*, 12–25. [CrossRef]
27. Kechiched, R.; Laouar, R.; Bruguier, O.; Salmi-Laouar, S.; Kocsis, L.; Bosch, D.; Foufou, A.; Ameur-Zaimeche, O.; Larit, H. Glauconite-bearing sedimentary phosphorites from the Tébessa region (eastern Algeria): Evidence of REE enrichment and geochemical constraints on their origin. *J. Afr. Earth Sci.* **2018**, *145*, 190–200. [CrossRef]
28. Wigley, R.; Compton, J.S. Oligocene to Holocene glauconite-phosphorite grains from the Head of the Cape Canyon on the western margin of South Africa. *Deep-Sea Res. Part II Top. Stud. Oceanogr.* **2007**, *54*, 1375–1395. [CrossRef]
29. Banerjee, S.; Choudhury, T.R.; Saraswati, P.K.; Khanolkar, S. The formation of authigenic deposits during Paleogene warm climatic intervals: A review. *J. Palaeogeogr.* **2020**, *9*, 27. [CrossRef]

30. Bezdeneznych, L.; Kharlamova, O.; Shmandiy, V.; Rigas, T. Research of adsorption properties of glauconite-based composite adsorbents. *J. Ecol. Eng.* **2020**, *21*, 147–154. [CrossRef]
31. Chayka, O.; Petrushka, I.; Ruda, M.; Paranyak, N.; Matskiv, O. The minimization of impact of oil pollution on soils in the area of railways using glauconite. *J. Water Land Dev.* **2021**, *49*, 79–84. [CrossRef]
32. Syrchina, N.V.; Pilip, L.V.; Ashikhmina, T.Y.; Kantor, G.Y. Effect of glauconite-containing wastes obtained during phosphorite enrichment on lead mobility in soils. *Biol. Bull.* **2022**, *3*, 350–360.
33. Sobeih, M.M.; El-Shahat, M.F.; Osman, A.; Zaid, M.A.; Nassar, M.Y. Glauconite clay-functionalized chitosan nanocomposites for efficient adsorptive removal of fluoride ions from polluted aqueous solutions. *RSC Adv.* **2020**, *10*, 25567–25585. [CrossRef] [PubMed]
34. El-mahllawy, M.S. An Investigation on the Effect of Cement Kiln Dust and Glauconite on the Properties of Acid Resisting Brick. *International Journalof Science and Technology Volume.* **2013**, *2*, 30–43.
35. Peregudov, Y.S.; Mezhri, R.; Gorbunova, E.M.; Niftaliev, S.I. Glauconite-based sorbents for oil and oil products collection. *Condens. Matter Interphases* **2020**, *22*, 257–265. [CrossRef]
36. Bushinsky, G.I. Petrography and some questions of genesis of Egorievsk phosphorites of Moscow Region. Bulletin of the Moscow Society of Nature Testers. *Dep. Geol.* **1937**, *15*, 438–471. (In Russian)
37. Salman, M.I.; Yashina, A.V. Geostatistical analysis of geological and industrial parameters of the Egorievsk field of gallstone phosphorites. *Min. Inf.-Anal. Bull.* **2006**, *7*, 110–115. (In Russian)
38. Kuzmin, A.N.N.; Kirikov, V.P.; Lukyanova, N.V.; Maksimov, A.V.; Kossovaya, I.O.; Evdokimova, N.R.; Gorbatsevich, V.V.; Savanin, G.V.; Kotlyar, A.V.; Samsonov. Savanin, G.V.; et al. *State Geological Map of the Russian Federation. Scale 1:1,000,000*, 3rd ed.; Central European Series. Sheet N-37—Moscow. Explanatory note.—St. Petersburg; Cartographic Factory VSEGEI: Saint Petersburg, Russia, 2015. (In Russian)
39. Lygach, A.V. State-of-the-art and prospects of using Egorievsk nodular phosphorite in the Voskresensky district, Moscow region. *Min. Inf. Anal. Bull.* **2018**, *2018*, 29–37. [CrossRef]
40. Lygach, A.V.; Ignatkina, V.A. Flotation properties of base minerals in Egorievsk nodular phosphorite. *Min. Inf. Anal. Bull.* **2018**, *2018*, 163–175. [CrossRef]
41. Moore, D.M.; Reynolds, R.C. *X-ray Diffraction and the Identification and Analysis of Clay Minerals*; Illinois: State Geologycal Survey; Oxford University Press: Oxford, UK, 1989; p. 332.
42. Bish, D.L.; Post, J.E. Quantitative mineralogical analysis using the Rietveld full-pattern fitting method. *Am. Mineral.* **1993**, *78*, 932–940.
43. Rudmin, M.; Banerjee, S.; Makarov, B.; Belousov, P.; Kurovsky, A.; Ibraeva, K.; Buyakov, A. Glauconite-Urea Nanocomposites As Polyfunctional Controlled-Release Fertilisers. *J. Soil Sci. Plant Nutr.* **2022**, *22*, 4035–4046. [CrossRef]
44. Paula De Souza, M.E.; Cardoso, I.M.; De Carvalho, A.M.X.; Lopes, A.P.; Jucksch, I.; Janssen, A. Rock Powder Can Improve Vermicompost Chemical Properties and Plant Nutrition: An On-farm Experiment. *Commun. Soil Sci. Plant Anal.* **2018**, *49*, 1–12. [CrossRef]
45. Westfall, D.G.; Mortvedt, J.J.; Peterson, G.A.; Gangloff, W.J. Efficient and Environmentally Safe Use of Micronutrients in Agriculture. *Commun. Soil Sci. Plant Anal.* **2005**, *36*, 169–182. [CrossRef]
46. *GOST R 58658-2019*; Products and Food with Improved Characteristics. Mineral Fertilisers. General Technical Conditions (with Amendments). Federal Agency for Technical Regulation and Metrology: Moscow, Russia, 2022. (In Russian)
47. Cakmak, I.; Yazici, A.M. Magnesium: A forgotten element in crop production. *Better Crops* **2010**, *94*, 23–25. Available online: https://www.ksminerals-and-agriculture.com/en/pdf-articles/article-201006-better-crops-magnesium.pdf (accessed on 27 August 2023).
48. Ishfaq, M.; Wang, Y.; Yan, M.; Wang, Z.; Wu, L.; Li, C.; Li, X. Physiological Essence of Magnesium in Plants and Its Widespread Deficiency in the Farming System of China. *Front. Plant Sci.* **2022**, *13*, 802274. [CrossRef]
49. Eskandari, H. The Importance of Iron (Fe) in Plant Products and Mechanism of Its Uptake by Plants. *J. Appl. Environ. Biol. Sci.* **2011**, *1*, 448–452.
50. Rout, G.R.; Sahoo, S. Role of iron in plant growth and metabolism. *Rev. Agric. Sci.* **2015**, *3*, 1–24. [CrossRef]
51. Shatagin, N.N.; Iranmanesh, M.; Fazlavi, A. An Estimation of Heavy Metals Environmental Impact from Phosphorites of Egorievsk Deposit (Moskow Region, Russia). In Proceedings of the 4th International Iran and Russia Conference "Agriculture and Natural Resources", Shahrekord, Iran, 8–10 September 2004; pp. 205–206.
52. Iranmanesh, M. Assessment of Environmental Impact of Toxic Metals from Phosphorites of Egorievsk Deposit (Moscow region, Russia). In Proceedings of the X International Environmental Conference of Students and Young Scientists "Environmental Safety as a Key Factor of Sustainable Development", Moscow, Russia, 25–27 April 2006. (In Russian).
53. Iranmanesh, M.; Shatagin, N.N.; Baraboshkina, T.A. Ecogeology of Phosphorite Deposits of the Moskovskaya Syneclise. In Proceedings of the V International Scientific and Practical Conference "Science and the Latest Technologies in the Search, Exploration and Development of Mineral Deposits", Dushanbe, Tajikistan, 12–15 June 2006; p. 011001. (In Russian).
54. Das, C.K.; Srivastava, G.; Dubey, A.; Roy, M.; Jain, S.; Sethy, N.K.; Saxena, M.; Harke, S.; Sarkar, S.; Misra, K.; et al. Nano-iron pyrite seed dressing: A sustainable intervention to reduce fertilizer consumption in vegetable (beetroot, carrot), spice (fenugreek), fodder (alfalfa), and oilseed (mustard, sesamum) crops. *Nanotechnol. Environ. Eng.* **2016**, *1*, 2. [CrossRef]

55. Ortas, I.; Kaya, Z.; Ercan, S. Effect of Pyrite Application on Wheat-Maize Growth and Nutrient Uptake Under Diverse Soil Conditions. *J. Plant Nutr.* **2015**, *38*, 295–309. [CrossRef]
56. Tiwari, K.N.; Dwivedi, B.S.; Pathak, A.N. Evaluation of iron pyrites as sulphur fertilizer. *Fertil. Res.* **1984**, *5*, 235–243. [CrossRef]
57. Guidry, M.W.; Mackenzie, F.T. Experimental study of igneous and sedimentary apatite dissolution. *Geochim. Cosmochim. Acta* **2003**, *67*, 2949–2963. [CrossRef]
58. Valsami-Jones, E.; Ragnarsdottir, K.V.; Putnis, A.; Bosbach, D.; Kemp, A.J.; Cressey, G. The dissolution of apatite in the presence of aqueous metal cations at pH 2–7. *Chem. Geol.* **1998**, *151*, 215–233. [CrossRef]
59. Zhenghua, W.; Xiaorong, W.; Yufeng, Z.; Lemei, D.; Yijun, C. Effects of apatite and calcium oxyphosphate on speciation and bioavailability of exogenous rare earth elements in the soil-plant system. *Chem. Speciat. Bioavailab.* **2001**, *13*, 49–56. [CrossRef]